

University of Wollongong

Research Online

Faculty of Engineering and Information
Sciences - Papers: Part A

Faculty of Engineering and Information
Sciences

January 2014

A BER based adaptive STFC MB-OFDM UWB system for WBAN applications

Miftadi Sudjai

University of Wollongong, ms917@uowmail.edu.au

Le Chung Tran

University of Wollongong, lctran@uow.edu.au

Follow this and additional works at: <https://ro.uow.edu.au/eispapers>

Research Online is the open access institutional repository for the University of Wollongong. For further information contact the UOW Library: research-pubs@uow.edu.au

A BER based adaptive STFC MB-OFDM UWB system for WBAN applications

Abstract

A bit error rate (BER) estimation-based adaptive space-time-frequency coded (STFC) multiband orthogonal frequency division multiplexing ultra-wideband (MB-OFDM UWB) wireless body area network (WBAN) system is proposed in this paper. It is designed to improve the average BER performance for high data rate applications while maintaining a reasonably high throughput in body-to-external links of a WBAN. The performance improvement fundamentally translates to power saving at the transmitter and/or receiver, thus reducing battery requirements and size of WBAN devices. Two novel blocks, namely the BER estimation-based adaptive algorithm which controls the set of modulation, STFC coding rate, and power of signal constellations, and the linearly interpolated CM4 WBAN channel model are implemented in the proposed adaptive STFC MB-OFDM UWB WBAN system. Three sets of adaptive schemes are defined, each of which is determined by two BER thresholds, i.e. the lower and upper thresholds, which are in turns calculated from the non-adaptive average BER performance as the benchmark. Simulation results show a significant improvement in the performance and/or Tx/Rx power saving, with the cost of a slight reduction in the throughput.

Keywords

ber, stfc, mb, adaptive, uwb, wban, system, ofdm, applications

Publication Details

M. Sudjai & L. Chung. Tran, "A BER based adaptive STFC MB-OFDM UWB system for WBAN applications," in IEEE International Conference on Communications (ICC), 2014, pp. 5670-5675.

A BER Based Adaptive STFC MB-OFDM UWB System for WBAN Applications

Miftadi Sudjai* and Le Chung Tran

School of Electrical, Computer, and Telecommunication Engineering

University of Wollongong, NSW 2522 Australia

Phone: +61 4 2605 8576, Fax: +61 2 4221 3236

*Email: ms917@uow.edu.au

Abstract—A bit error rate (BER) estimation-based adaptive space-time-frequency coded (STFC) multiband orthogonal frequency division multiplexing ultra-wideband (MB-OFDM UWB) wireless body area network (WBAN) system is proposed in this paper. It is designed to improve the average BER performance for high data rate applications while maintaining a reasonably high throughput in *body-to-external* links of a WBAN. The performance improvement fundamentally translates to power saving at the transmitter and/or receiver, thus reducing battery requirements and size of WBAN devices. Two novel blocks, namely the BER estimation-based adaptive algorithm which controls the set of modulation, STFC coding rate, and power of signal constellations, and the linearly interpolated CM4 WBAN channel model are implemented in the proposed adaptive STFC MB-OFDM UWB WBAN system. Three sets of adaptive schemes are defined, each of which is determined by two BER thresholds, i.e. the lower and upper thresholds, which are in turns calculated from the non-adaptive average BER performance as the benchmark. Simulation results show a significant improvement in the performance and/or Tx/Rx power saving, with the cost of a slight reduction in the throughput.

Keywords— Adaptive system, MIMO, UWB, WBAN

I. INTRODUCTION

Attracted by a wide range of potential applications, such as for entertainment, military, and health care, wireless body area networks (WBANs) have become one of the main research streams during the last several years [7]. The capability of WBAN system to wirelessly interconnect body centric devices opens up possibilities of new technology such as implantable and wearable sensors and transceiver to monitor internal organs and health conditions. To push forward the implementation and commercialization of WBAN systems, IEEE has established an impulse radio ultra wideband (IR-UWB) based WBAN standard in 2012 [3]. However, the standard only supports the maximum data rate up to 15.6 Mbps with a bandwidth of 499 MHz.

Another competing technology for a WBAN system is MB-OFDM UWB endorsed by the WiMedia Alliance [1]. It is capable to support much higher data rate up to 1 Gbps. Thus, in [8], we proposed the use of MB-OFDM UWB as an physical layer for *high data rate* WBANs, in combination with Space-Time-Frequency Coded Multi-Input Multi-Output (STFC MIMO) techniques. We demonstrated that the proposed system, referred to as STFC MB-OFDM UWB,

could provide better performance at higher data rate with the price of a modest increase in complexity. Hence, this work is mainly based on the system defined in [8] and [9].

The WBAN channel models have been published by IEEE [5]. It defines four different channel models (CM1 – CM4), where CM4 considers the *body-to-external* link and is of our interest in this paper. The CM4 takes into account body directions toward a transmitter. The CM4 determines different propagation channels for four discrete body directions 0° , 90° , 180° , and 270° . To make a finer CM4 channel modeling, herein we develop a linear interpolation of the CM4 with 1° resolution, instead of 90° as above. The interpolated CM4 channel model is used to investigate performance and throughput of the adaptive WBAN system.

Adaptive techniques have been employed for numerous applications. Czylik [2], for instance, proposed an adaptive modulation for individual subcarriers of an OFDM. Keller and Hanzo investigated adaptive OFDM with the focus on trade-off between the performance and throughput [15]. They also provided an array of adaptive OFDM techniques and their performances [16]. In [13], the authors examined a unified adaptive modulation approach where the data rate, transmitted power, and instantaneous BER are varied to maximize spectral efficiency. The authors in [4] proposed a simple adaptive channel estimation scheme for MB-OFDM UWB system for WPAN (Wireless Personal Area Network) applications. However, the performance improvement is not significant. Fu, *et al.* proposed a link adaptation scheme for MB-OFDM UWB systems [10]. Nevertheless, the adaptive system for the WBAN has been almost unexplored in the literature. Thus in [9], we proposed, a simple but practical, angular body direction-based adaptive algorithm implemented in STFC MB-OFDM UWB WBAN. However, the performance as well as the adaptive algorithm needs to be improved further to obtain better results, and is addressed in this paper.

Apart from the aforementioned contribution of the linear interpolation of CM4 channel model, this paper proposes a BER estimation-based adaptive algorithm implemented for STFC MB-OFDM UWB WBAN system. The core idea is that a combination of different digital modulation schemes (BPSK, QPSK), powers of signal constellations, and STFC coding rates is adaptively selected, depending on the quality of the channel (in terms of BER). The objective is to achieve better performance for high data rate WBAN applications while

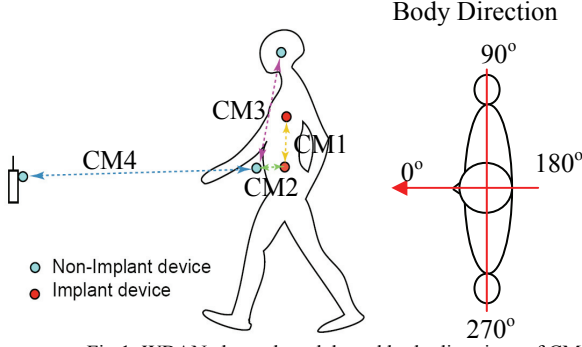


Fig.1. WBAN channel models and body directions of CM4 [6].

maintaining a reasonably high throughput. The improvement is translated to Tx/Rx power saving to minimize the power requirement of WBAN devices. Simulations show a significant performance improvement and/or Tx/Rx power saving in the order of 1-8 dB depending on the MIMO configuration, with a minor reduction in the throughput. In addition, an optimization of adaptive parameters will be put forward to improve the trade-off between the performance and throughput in our future works.

The paper is organized as follows. Section II describes our proposed interpolated CM4 channel model. Section III describes transmission system and adaptive scheme, including the decoding complexity. Simulation results and analyses are presented in Section IV. Section V concludes the paper.

II. PROPOSED CHANNEL LINEAR INTERPOLATION

A. Review of IEEE's CM4 WBAN Channel Model

IEEE's CM4 WBAN channel model [5] for a *body surface-to-external* WBAN link is depicted in Fig.1. One of its three designated frequency bands is UWB band (3.1-10.6 GHz). The channel model takes into account the effect of body directions.

The CM4 channel response is characterized by the following power delay profile:

$$h(t) = \sum_{m=0}^{L-1} \alpha_m \delta(t - \tau_m) \quad (1)$$

where $|\alpha_m|^2 = \Omega_0 e^{-\frac{\tau_m}{T}} - k[1 - \delta(m)] \beta$

$$k = \Delta k \left(\frac{\ln 10}{10} \right); \tau_0 = d/c; \text{ and } \beta \sim \log \text{ normal}(0, \sigma).$$

L is the number of arrival paths, modeled as a Poisson random variable with the mean value of 400; α_m is the amplitude of each path; τ_m , $m = 1, \dots, L-1$, is timing of path arrivals and is modeled as a Poisson random process with the arrival rate $\lambda = 1/0.501251$ ns; Γ is an exponential decay factor with Ω_0 as the path loss; k is the K-factor (NLOS), d is the Tx-Rx distance, and c is the velocity of light. The CM4 also depends on the direction of body toward the Tx antenna, and listed in Table I.

TABLE I. PARAMETERS OF CM4 [6].

Body Direction	Γ (ns)	k (Δk (dB))	σ (dB)
0°	44.6364	5.111(22.2)	7.30
90°	54.2868	4.348(18.8)	7.08
180°	53.4186	3.638(15.8)	7.03
270°	83.9635	3.983(17.3)	7.19

B. Proposed Interpolation of CM4 WBAN Channel Model

Linear interpolation of CM4 as in Fig.2 is conducted to acquire a 1° resolution, instead of 90° resolution as originally defined in [5] and [14]. It is determined by a factor of $\left(\frac{b-q}{90}\right)$, where b is actual body direction, and q is 0°, 90°, 180°, or 270°. Three parameters, namely Γ , k , and σ are linearly interpolated by the formulas as below, where Γ_q , k_q , and σ_q are exponential decay factor, effect of K-factor (NLOS) k , and standard deviation values of q body direction as defined in the second column of Table I. It will produce approximate propagation characteristics of CM4 WBAN channel for every single body direction.

$$\begin{aligned}
 &0^\circ \leq b \leq 90^\circ: \quad \begin{cases} \Gamma = \Gamma_0 + (\Gamma_{90} - \Gamma_0) \times \left(\frac{b}{90}\right) \\ k = k_0 + (k_{90} - k_0) \times \left(\frac{b}{90}\right) \\ \sigma = \sigma_0 + (\sigma_{90} - \sigma_0) \times \left(\frac{b}{90}\right) \end{cases} \\
 &90^\circ \leq b \leq 180^\circ: \quad \begin{cases} \Gamma = \Gamma_{90} + (\Gamma_{180} - \Gamma_{90}) \times \left(\frac{b-90}{90}\right) \\ k = k_{90} + (k_{180} - k_{90}) \times \left(\frac{b-90}{90}\right) \\ \sigma = \sigma_{90} + (\sigma_{180} - \sigma_{90}) \times \left(\frac{b-90}{90}\right) \end{cases} \\
 &180^\circ \leq b \leq 270^\circ: \quad \begin{cases} \Gamma = \Gamma_{180} + (\Gamma_{270} - \Gamma_{180}) \times \left(\frac{b-180}{90}\right) \\ k = k_{180} + (k_{270} - k_{180}) \times \left(\frac{b-180}{90}\right) \\ \sigma = \sigma_{180} + (\sigma_{270} - \sigma_{180}) \times \left(\frac{b-180}{90}\right) \end{cases} \\
 &270^\circ \leq b \leq 360^\circ: \quad \begin{cases} \Gamma = \Gamma_{270} + (\Gamma_0 - \Gamma_{270}) \times \left(\frac{b-270}{90}\right) \\ k = k_{270} + (k_0 - k_{270}) \times \left(\frac{b-270}{90}\right) \\ \sigma = \sigma_{270} + (\sigma_0 - \sigma_{270}) \times \left(\frac{b-270}{90}\right) \end{cases}
 \end{aligned}$$

Fig.2. Interpolation of IEEE CM4 WBAN channel.

III. PROPOSED ADAPTIVE STFC MB-OFDM UWB SYSTEM

A. System Model

Fig.3 depicts the proposed adaptive STFC MIMO-OFDM UWB WBAN system with M -Tx antennas and N -Rx antennas. The data stream $d(n)$ is convolutionally coded and interleaved before being mapped to symbols. The BER estimator measures the channel quality, compares it with the preset thresholds, and then decides which adaptive scheme *Set-j* to be employed and fed back to the transmitter in order to adjust its modulation, constellation power, and STFC coding rate. The adaptive modulation block selects either QPSK or BPSK, while power control block adjusts the power. The stream of modulated symbols is then converted by a Serial-to-Parallel (S/P) block into the symbol blocks (or vectors) $\bar{x} = [x_1, x_2, \dots, x_{N_{fft}}]^T$, where N_{fft} is the FFT/IFFT size.

The adaptive STFC block creates a space-time code with either full rate, or 3/2-rate. The full rate uses the Alamouti code [11] to convert the two consecutive symbol blocks, into a STFC block as follows

$$\mathbf{X} = \{\bar{x}_{t,m}\}_{T \times M} = \begin{bmatrix} \bar{x}_1 & \bar{x}_2 \\ -\bar{x}_2^* & \bar{x}_1^* \end{bmatrix} \quad (2)$$

where \bar{x}_1 and \bar{x}_2 are symbol vectors transmitted from the first and the second antenna at a given time slot, respectively. $(.)^*$ denotes complex conjugate. For 3/2-rate STFC, three symbol vectors are encoded following the Sezginer-Sari code [12]

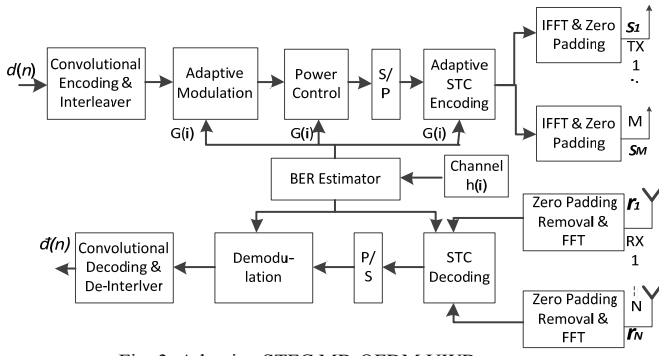


Fig. 3. Adaptive STFC MB-OFDM UWB system

$$\mathbf{X} = \{\bar{x}_{t,m}\}_{T \times M} = \begin{bmatrix} a\bar{x}_1 + \frac{b\bar{x}_3}{\sqrt{2}} & -\left(c\bar{x}_2^* + \frac{d\bar{x}_3^*}{\sqrt{2}}\right) \\ a\bar{x}_2 + \frac{b\bar{x}_3}{\sqrt{2}} & c\bar{x}_1^* + \frac{d\bar{x}_3^*}{\sqrt{2}} \end{bmatrix} \quad (3)$$

where a , b , c , and d are complex-valued design parameters. Here, we use the optimum parameters $a = c = \sqrt{2}$, and $b = d = (1 + j\sqrt{7})/4$ as determined in [12].

We denote the matrix $\mathbf{X} = \{\bar{x}_{t,m}\}_{T \times M}$, where t indicates the time slot and m indicates the Tx antenna. Each of symbol vectors in the matrix \mathbf{X} is converted into an N_{fft} -point STFC MB-OFDM symbol by the IFFT block, resulting in the matrix

$$\mathbf{X}_{OFDM} = \{\bar{x}_{OFDM,t,m}\}_{T \times M} = \{\text{IFFT}\{\bar{x}_{t,m}\}\}_{T \times M} \quad (4)$$

The transmitted matrix is the matrix \mathbf{X}_{ZP} whose elements are elements of \mathbf{X}_{OFDM} appended with the 37-samples zero padded suffix (ZPS), denoted as $\bar{x}_{ZP,t,m}$. This means

$$\mathbf{X}_{ZP} = \{\bar{x}_{ZP,t,m}\}_{T \times M} \quad (5)$$

The channels between M -Tx antennas and N -Rx antennas are defined as the channel matrix \mathbf{H}

$$\mathbf{H} = \begin{bmatrix} \bar{h}_{1,1} & \cdots & \bar{h}_{M,1} \\ \vdots & \ddots & \vdots \\ \bar{h}_{1,N} & \cdots & \bar{h}_{M,N} \end{bmatrix} \quad (6)$$

where $\bar{h}_{m,n}$ is the channel coefficient vector between the m -th Tx antenna, for $m = 1, 2, \dots, M$, and the n -th Rx antenna, $n = 1, 2, \dots, N$, containing L multipath. The distribution and parameters of $\bar{h}_{m,n}$ are determined by Eq. (1) and Table I.

The received signal at the n -th Rx antenna during the t -th transmitted OFDM symbol duration is computed as

$$\bar{r}_{t,n} = \sum_{m=1}^M (\bar{x}_{ZP,t,m} \otimes \bar{h}_{m,n}) + \bar{n}_{t,n} \quad (7)$$

where \otimes denotes the *linear convolution*, and $\bar{n}_{t,n}$ is the zero mean additive white Gaussian noise vector. The ZPS is removed by an Overlap-And-Add-Operation (OAAO) prior to FFT operation, hence the received signal can be written as [6]

$$\bar{r}_{OFDM,t,n} = \sum_{m=1}^M \bar{x}_{OFDM,t,m} * \bar{h}_{m,n} + \bar{n}_{t,n} \quad (8)$$

where $*$ denotes *circular convolution*. After the FFT block, input signals of the STFC decoder is calculated as [6, Eq.(12)]

$$\bar{r}_{t,n} = \sum_{m=1}^M \bar{x}_{t,m} \cdot \bar{h}_{m,n} + \bar{n}_{t,n} \quad (9)$$

where (\cdot) denotes the dot (Hardamard) product between the two vectors, $\bar{r}_{t,n} = \text{FFT}(\bar{r}_{OFDM,t,n}) = [\bar{r}_{m,n,1}, \dots, \bar{r}_{m,n,N_{fft}}]^T$, $\bar{x}_{t,m}$ is the original modulation symbols, $\bar{h}_{m,n} = \text{FFT}(\bar{h}_{mn}) = [\bar{h}_{m,n,1}, \dots, \bar{h}_{m,n,N_{fft}}]^T$, and $\bar{n}_{t,n} = \text{FFT}(\bar{n}_{t,n})$. Denote $\mathcal{R} = \{\bar{r}_{t,n}\}_{T \times N}$ to be the matrix of the received signals after FFT, $\mathcal{H} = \{\bar{h}_{m,n}\}_{M \times N}$ to be the channel response matrix, and $\mathcal{N} = \{\bar{n}_{t,n}\}_{T \times N}$ the matrix of noise. Then we can re-write (9) as

$$\mathcal{R} = \mathbf{X} \circ \mathcal{H} + \mathcal{N} \quad (10)$$

where (\circ) denotes the operation which is similar to the normal matrix multiplication, except that each element in \mathcal{R} is determined by (9). Thus the detected vectors are decided by the following Maximum Likelihood (ML) rule

$$\{\tilde{\bar{x}}_{t,m}\} = \arg \min_{\{\bar{x}_{t,m}\}} \|\mathcal{R} - \mathbf{X} \circ \mathcal{H}\|_F^2 \quad (11)$$

Since the matrix \mathbf{X} preserves its orthogonality in the similar manner as in a conventional STBC (Space-Time Block Code) MIMO system, the STFC MB-OFDM UWB system can also employ a simple linear decoding process. For simplicity, we can omit the time index t . Hence in the 2I1O configuration with M-PSK modulation, we have the following decoding metrics

$$\bar{x}_1 = \arg \min_{\bar{x} \in \mathcal{C}^{N_D}} \|(\bar{h}_1^* \cdot \bar{r}_1 + \bar{h}_2 \cdot \bar{r}_2^*) - \bar{x}\|_F^2 \quad (12)$$

$$\bar{x}_2 = \arg \min_{\bar{x} \in \mathcal{C}^{N_D}} \|(\bar{h}_2^* \cdot \bar{r}_1 - \bar{h}_1 \cdot \bar{r}_2^*) - \bar{x}\|_F^2$$

where N_D is number of data subcarriers, and \mathcal{C}^{N_D} denotes the N_D -dimensional complex space of the transmitted vector \bar{x} . More importantly, each data point in an MB-OFDM symbol can be decoded separately rather than jointly, thus the decoding process is significantly simplified [6]. The decoding metric of each data at the k -th subcarrier ($k=1, \dots, N_D$) in the MB-OFDM symbols for the 2I1O configuration are

$$\begin{aligned} \tilde{x}_{1,k} &= \arg \min_{x_{1,k} \in \mathcal{C}} \left[|(\bar{h}_{1,k}^* \bar{r}_{1,k} + \bar{h}_{2,k} \bar{r}_{2,k}^*) - x_{1,k}|^2 \right] \\ \tilde{x}_{2,k} &= \arg \min_{x_{2,k} \in \mathcal{C}} \left[|(\bar{h}_{2,k}^* \bar{r}_{1,k} - \bar{h}_{1,k} \bar{r}_{2,k}^*) - x_{1,k}|^2 \right] \end{aligned} \quad (13)$$

Similarly, for the 2I2O configuration, the decoding metrics are

$$\begin{aligned} \tilde{x}_{1,k} &= \arg \min_{x_{1,k} \in \mathcal{C}} \left[\left| \sum_{n=1}^2 (\bar{h}_{1,n,k}^* \bar{r}_{1,n,k} + \bar{h}_{2,n,k} \bar{r}_{2,n,k}^*) - x_{1,k} \right|^2 \right] \\ \tilde{x}_{2,k} &= \arg \min_{x_{2,k} \in \mathcal{C}} \left[\left| \sum_{n=1}^2 (\bar{h}_{2,n,k}^* \bar{r}_{1,n,k} - \bar{h}_{1,n,k} \bar{r}_{2,n,k}^*) - x_{2,k} \right|^2 \right] \end{aligned} \quad (14)$$

For the 3/2-rate STFC, we follow the decoding process as mentioned in [12]. Generalization for the case of M -Tx and N -Rx antennas is straightforward.

B. Transmission Model and Adaptive Algorithms

The aforementioned interpolated CM4 WBAN channel with 1° resolution is used for channel realization. For the ease of illustration, it is assumed that a person wearing the WBAN devices turns the body (Rx) clock-wisely against transmitter. With regard to the angular movement of the body, Tx transmits one superframe in each 15° of body direction.

The selection of the adaptive scheme *Set-j*, where $j = 1, 2$, and 3 , is done in a way that the average throughput and total transmitted power, assuming an equal probability of each *Set-j* to occur, are maintained exactly equal to those in a non-adaptive system for a fair comparison. Here, the non-adaptive system employs QPSK, STFC code rate 1.0, and power 1.0, providing a spectral density of 2 bps/Hz.

Three adaptive schemes are defined. *Set-1*, is aimed to take advantage of the best channel link by maximizing the throughput, i.e. by employing QPSK modulation, STFC code rate $3/2$ and normalized transmission power 1.5, providing a spectral density of 3 bps/Hz. *Set-2* is used for the average channel condition, hence employs the same scheme as the non-adaptive system. *Set-3* is designed to tackle the worst channel condition by employing more powerful BPSK modulation, STFC code rate 1.0, and power 0.5, providing a spectral density of 1 bps/Hz.

Transmission model is depicted in Fig.4. *Set-2* is always used in the first part of each superframe which makes up a portion, denoted as f , ($0 < f < 1$), of that superframe. The receiver measures the quality of the channel, i.e. BER, for this portion, compares it to the preset thresholds (discussed in the next section), and then decides which *Set-j* to be fed back to the transmitter to update the adaptive scheme for the remaining portion ($1-f$) of that superframe. Note that the information of *Set-j* does not require to be transmitted to the receiver, since it already knows what adaptive *Set-j* will be used in the remaining of the superframe when it compares the BER with the preset thresholds. Upon completion of transmission of a superframe, the first portion f of the next superframe will use *Set-2* again, followed by the same procedure as above.

C. Preset BER Thresholds

The adaptive scheme is controlled by the measurement of the quality of signal at Rx, i.e. BER, and compared to the BER thresholds. Two BER thresholds are defined, i.e. upper and lower thresholds that determine the selection of one of three possible schemes of *Set-j*. The upper and lower thresholds are derived from the non-adaptive average BER performance as the benchmark.

Two methods are used to define the preset thresholds that trigger the change of adaptive schemes, namely linear and non-linear BER thresholds. The linear BER thresholds define a constant deviation for the whole range of SNR w.r.t. to the non-adaptive average BER performance as the benchmark. The lower and upper linear thresholds are defined as follows

$$BER_{L,l}^{(i)} = BER_{NA}^{(i)} - k_1 \times BER_{NA}^{(i)} \quad (15)$$

$$BER_{U,l}^{(i)} = BER_{NA}^{(i)} + k_2 \times BER_{NA}^{(i)} \quad (16)$$

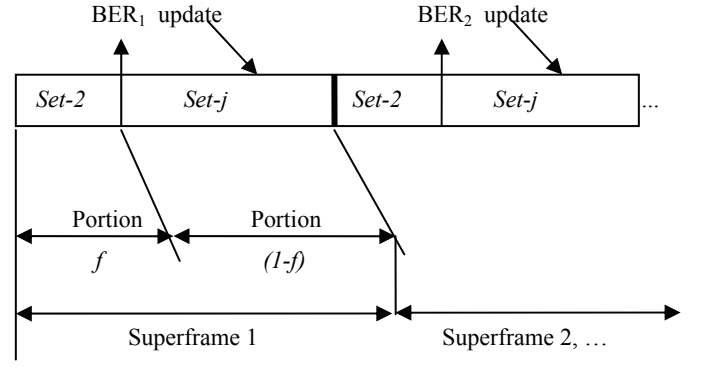


Fig.4. Transmission model in the proposed adaptive scheme.

where $BER_{L,l}^{(i)}$ is the lower threshold, $BER_{U,l}^{(i)}$ is the upper threshold, and $BER_{NA}^{(i)}$ is the non-adaptive average BER performance for i -th SNR value. k_1 and k_2 are constants. The subscript l denotes the linear threshold approach, and index i is an integer representing steps in the SNR increment.

The non-linear BER thresholds define a smaller deviation in the low SNR w.r.t. to the non-adaptive average BER performance, and the deviation is non-linearly increased when the SNR increases. It is done in order to allow higher probability of *Set-1* to occur, resulting in a higher throughput when the channel condition is better (higher SNR). The lower and upper non-linear thresholds are defined as follows:

$$BER_{L,nl}^{(i)} = BER_{NA}^{(i)} - k_3 \times BER_{NA}^{(i)} \times (1+p)^i \quad (17)$$

$$BER_{U,nl}^{(i)} = BER_{NA}^{(i)} + k_4 \times BER_{NA}^{(i)} \times (1+p)^i \quad (18)$$

where p is a non-linear factor, and k_3 and k_4 are constants. The subscript nl denotes the non-linear threshold approach.

The proposed algorithm for each superframe transmission is summarized as follows:

```

Start
Measure BER in the initial portion;
If BER < BERL
    Set_Modulation = qpsk;
    Set_Power_Tx = 1.5;
    Set_STFC_rate = 1.5;
} Use Set-1 for the remaining of superframe
If BER ≥ BERL and BER ≤ BERU
    Set_Modulation = qpsk;
    Set_Power_Tx = 1.0;
    Set_STFC_rate = 1.0;
} Use Set-2
else
    Set_Modulation = bpsk;
    Set_Power_Tx = 0.5;
    Set_STFC_rate = 1.0;
} Use Set-3
End

```

D. Complexity Analyses

The decoding process of the $3/2$ rate code has the complexity $O(4)$ compared with the full rate code, since the decoder firstly has to decide \tilde{x}_3 from four possible symbols in QPSK, prior to decoding \tilde{x}_1 and \tilde{x}_2 symbols. Meanwhile, in the worst link, the complexity is reduced to $O(2)$ due to BPSK

(rather than QPSK) is used. The overall complexity of the decoding process increases by a factor of $[O(4)-O(2)]$, beside the BER estimator. It should be emphasized that, though the decoding complexity in the adaptive system increases, the decoding processes for both adaptive and non-adaptive system are relatively simple.

As previously mentioned, the measured BER is not fed back directly to the transmitter. Instead, it will be compared to the preset thresholds with the outcome of one out of three possible set of adaptive schemes *Set-j*. Hence, only two bits are required to be fed back to the transmitter to indicate which set of adaptive scheme to be used. In other words, the proposed adaptive scheme could be implemented with only a slight increase in system complexity.

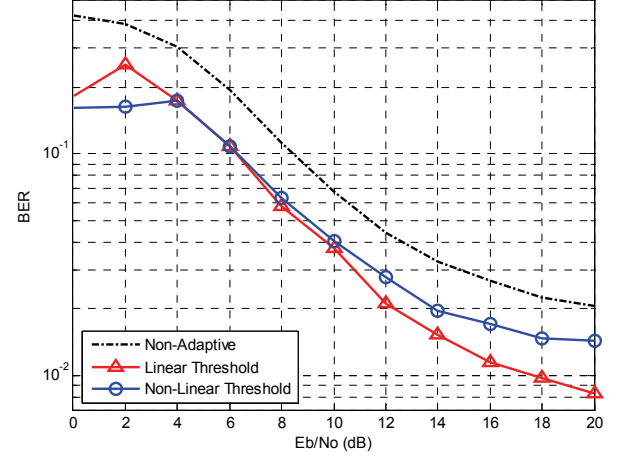
IV. SIMULATION RESULTS

The simulations are conducted to compare the average BER and throughput of the adaptive system with the non-adaptive one, assuming perfect channel state estimations are available at the receiver. The non-adaptive system uses *Set-2* for all body directions, with average normalized throughput of 2 bps/Hz. The Tx sends one superframe for every 15° angular movement of the body. The simulations measure 24 superframes transmission over 24 different body directions that are equally spaced 15° from each others for every SNR point. Channel coefficients are assumed to be constant during each STFC block, but random between consecutive STFC blocks. The channel realizations are created based on our interpolated CM4 model. We set the portion of superframe $f = 25\%$, $p = 0.175$, $k_1 = k_2 = 0.7$, $k_3 = 0.15$ and $k_4 = 0.4$, respectively. Other simulation parameters are listed in Table II.

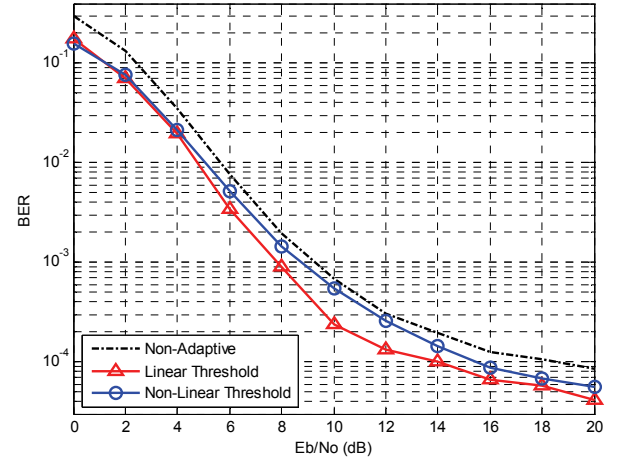
Fig.5 shows the average performance of the adaptive system for both 2I1O (a) and 2I2O (b) MIMO configuration, compared to the average non-adaptive system performance. The triangular line curve shows the performance of linear BER threshold, and the circled line curve shows the performance of non-linear BER threshold. Both of the BER thresholds approaches perform better than the non-adaptive system. In the 2I1O configuration, the improvement in the order of 3 – 6 dB is achieved by non-linear BER threshold, and of 3 – 8 dB by the linear BER threshold from low to medium SNR in which most of the WBAN system will be expected to operate. These gains show a significant improvement for WBAN applications. This proposed adaptive system could potentially save Tx/Rx power at a level of 50% - 85%, compared to the non-adaptive system. With this level of power reduction, the adaptive STFC MB-OFDM UWB system could be an energy efficient alternative for high data rate

TABLE II. SIMULATION PARAMETERS.

Parameters	Value
FFT & IFFT size N_{fft}	128
Number of ZPS N_{ZPS}	37
Convolutional coder (K=7) rate	$\frac{1}{2}$
Conv. decoder and mode	Viterbi, Hard
Interleaver/De-interleaver	Column-wise written, row-wise read
Average number of paths in CM4	400



(a)



(b)

Fig.5. Performances of the proposed adaptive schemes in CM4, (a) 2I1O, (b) 2I2O.

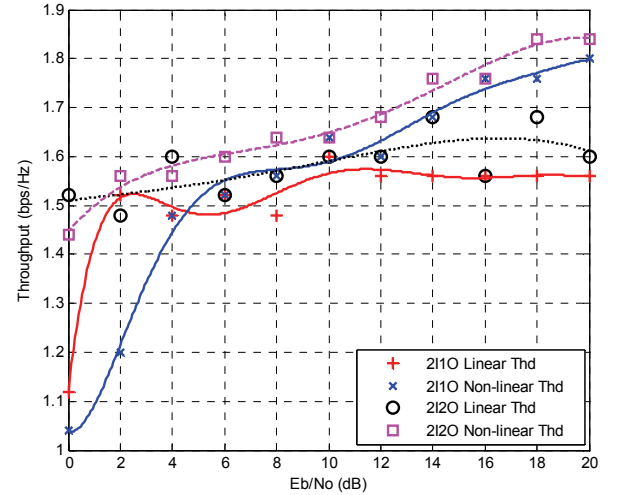


Fig.6. Normalized throughput of adaptive scheme in CM4.

WBAN applications. It is important to highlight the capability of this adaptive WBAN to offer much higher data rate, i.e. 1 Gbps, compared to Impulse Radio (IR) UWB based WBAN system whose maximum data rate is 15.6 Mbps [3].

From Fig.5, one can also see that the adaptive system with a 2I2O configuration provides a less improvement over the non-adaptive one, compared to the 2I1O configuration. The gain is around 1-4 dB or 20% - 60% TX/Rx power saving for the linear BER threshold. The non-linear BER threshold performs slightly better than the non-adaptive system in the whole SNR region. The improvement is smaller in the 2I2O configuration since the system already has a large number of diversity, so even the non-adaptive WBAN system could take advantage of it. Nonetheless, if we compare the error performance of the 2I1O and 2I2O configurations with each other, it is intuitive that the application of the proposed adaptive schemes in the 2I2O configuration provides better link quality up to BER of 10^{-5} that suits to more stringent QoS applications. However, it incurs a higher complexity in the hardware implementation.

The average normalized throughput taken from 24 different body directions are shown in Fig.6. The throughput is basically determined by the statistic of the measured BER in the receiver and depending on the channel condition in those body directions. The delays between the channel quality measurement, feedback link, and superframe transmission are negligible since the distance between Tx-Rx is around 2 – 10 m in *body-to-external* WBAN link. Hence, the throughput is not affected by those delays.

At low SNRs, *Set-3* with a lower spectral efficiency is most likely employed, resulting in a lower throughput for both linear and non-linear BER thresholds. At high SNR values, higher spectral efficiency adaptive schemes, i.e. *Set-1* and *Set-2*, are employed more frequently, leading to a higher throughput which approaches the non-adaptive throughput of 2 bps/Hz. However, the gap between the non-adaptive and adaptive throughputs is still significant, even at the high SNR. It is understandable since the adaptive scheme measures the BER of the most recently received portion f of a superframe in order to predict the link quality of the current uplink channel, and uses this information to assign a new adaptive scheme for the rest of the superframe. In addition, the selection of BER threshold parameters also affects the throughput and performance. However, overall, the results show that the aim as stated earlier has been fulfilled, i.e. gaining better performance for high data rate WBAN applications with a reasonably high throughput.

From Fig. 6, one can realize that, within the E_b/N_0 range [0-4] dB for 2I1O and [0-2] dB for 2I2O, the linear BER threshold approach tends to have higher throughput compare to the non-linear BER threshold. Thus, its BER performance within these ranges is slightly worse than that of the non-linear BER threshold approach. This slight performance difference between the two approaches can be seen clearly in Fig. 5.

Further adjustment of the adaptation or BER threshold parameters can possibly achieve better average throughput, while retaining good performance.

V. CONCLUSION

We have proposed a novel BER estimation-based adaptive STFC MB-OFDM UWB WBAN system aimed to improve the average BER performance while maintaining reasonably high throughput. It is shown that the adaptive system provide improvement in the order of 3 – 8 dB with 2I1O MIMO configuration, which practically means a 50% - 85% possible Tx/Rx power reduction, compared to the non-adaptive one. Meanwhile, the improvement of order 1-4 dB can be achieved by the 2I2O configuration. Those improvements come with a cost of minor reduction in the throughput. However, because of very high data rate capacity offered by the scheme, the throughput reduction is negligible, compared to what the existing standard can offer. With this capability, the adaptive STFC MB-OFDM UWB system could be an energy efficient alternative for high data rate WBAN applications. Our future work will focus on the optimization of adaptive parameters in an effort to further improve the performance and throughput.

REFERENCES

- [1] A. Batra *et al.*, "Multiband OFDM physical layer specification," *WiMedia Alliance*, Final Deliverable 1.5, Aug. 2009.
- [2] A. Czylik, "Adaptive OFDM for wideband radio channel", *Proc. GLOBECOM '96*, vol. 1, pp. 713-718, Nov. 1996.
- [3] IEEE Computer Society, "IEEE standard for local and metropolitan area networks-Part 15.6: Wireless Body Area Networks", Feb. 2012.
- [4] KB. Png, X. Peng, and F. Chin, "A low-complexity adaptive channel estimation scheme for MB-OFDM system", *Proc. Of ICUWB 2008*, vol.3, pp. 47-50, Sep. 2008.
- [5] K.Y. Yazdandoost and K. Sayrafi-Pour, "Channel model for Body area network (BAN)", *IEEE P802.15-08-0780-12-0006*, Nov. 2010.
- [6] L.C. Tran and A. Mertins, "Space-Time-Frequency Code implementation in MB-OFDM UWB communications: design criteria and performance", *IEEE Trans. Wireless Communication*, vol. 8, no. 2, Feb. 2009.
- [7] M. Chen, *et al.*, "Body Area Networks: A Survey", *Springer Journal on Mobile Netw Appl*, vol. 16, no. 2, pp.171-193, Aug. 2010.
- [8] M. Sudjai, L.C.Tran, and F. Safaei, "Performance analysis of STFC MB-OFDM UWB in WBAN channels", *Proc. 23rd IEEE PIMRC'12*, pp. 1704-1709, Sept. 2012.
- [9] M. Sudjai, L.C.Tran, and F. Safaei, "A simple adaptive STFC MB-OFDM UWB system for WBAN applications", *accepted to the 13th ISCIT-2013 Conference*, Sept. 2013.
- [10] S. Fu, D. Wang, H. Zhai, and Y. Li, "An enhanced link adaptation for the MB-OFDM UWB system", *Proc. IEEE WCNC'12*, pp. 2070-2075, Apr. 2012.
- [11] S. M. Alamouti, "A simple transmit diversity technique for wireless communications," *IEEE Journal on Selected Areas in Communications*, vol. 16, no. 8, pp. 1451-1458, Oct. 1998.
- [12] S. Sezginer and H. Sari, "A High-Rate Full-Diversity 2x2 Space-Time Code with simple Maximum Likelihood decoding", *Proc. ISSPIT'07*, pp. 1132-1136, Dec. 2007.
- [13] S. T. Chung and A.J. Goldsmith, "Degrees of freedom in adaptive modulation: a unified view", *IEEE Trans. On Commun.*, Vol. 49, No. 9, pp. 1561- 1571, Sep. 2001.
- [14] T. Aoyagi *et al.*, "Channel Models between body surface and wireless access point for UWB Band", *IEEE P802.15-08-0576-00-0006*, Aug. 2008.
- [15] T. Keller, and L. Hanzo, "Adaptive modulation techniques for duplex OFDM transmission", *IEEE Trans. Vehic. Tech.*, vol. 49, no. 5, Sept. 2000.
- [16] T. Keller, and L. Hanzo, "Adaptive multicarrier modulation: a convenient superframework for Time-Frequency processing in wireless communication", *Proceedings of the IEEE*, vol. 88, No.5, May 2000.